Supporting Information

Glucose-Responsive Magnetic Microrobots: 4D Printing and Targeted Embolization Application

Tong Lan[a], Qiong Wu[a], Chengyong Zhao[a], Haoyu Li[a], Jianguo Guan[a] and Fangzhi Mou*[a]

[a.] State Key Laboratory of Advanced Technology for Materials Synthesis and Processing, International School of Materials Science and Engineering, Wuhan University of Technology, Wuhan 430070, China

1. Experimental Section

1.1 Materials

Tetrabutylphosphonium chloride (80%, aqueous solution), acrylamide (AAM, 99%), 3-acrylamidophenylboronic acid (AA-PBA, 98%), N,N'-methylenebisacrylamide (BIS, 99%), polyvinylpyrrolidone (PVP, K30), 7-diethylamino-3-thiophen-2-yl-coumarin (DETC, 97%), glucose (99%), bovine serum albumin (BSA, 98%), and 3-(trimethoxysilyl)propyl methacrylate (MPS, 97%) were all purchased from Shanghai Macklin Biochemical Co., Ltd. PEGylated superparamagnetic Fe_3O_4 nanoparticles (NPs, 20 nm, 2.5%) were obtained from Jiangsu Zhichuan Technology Co., Ltd. Phosphate-buffered saline (PBS) and fetal bovine serum (FBS) were supplied by Biosharp Life Sciences Co., Ltd. Anhydrous ethanol, isopropanol, n-hexane, and acetic acid (all analytical grade) were purchased from China National Pharmaceutical Group Chemical Reagent Co., Ltd. All reagents were used as received without further purification.

1.2 Preparation of Magnetic Hydrogel inks

Various ratios of AAM, AA-PBA, BIS, and PVP were added to a fixed amount of 15 mg of DETC and 400 mg of tetrabutylphosphonium chloride (80 wt%, dissolved in ultrapure water). The mixture was homogenized using a probe-type ultrasonic

processor until fully dissolved, yielding the glucose-responsive hydrogel precursor solution. Subsequently, Fe_3O_4 NPs were introduced and ultrasonically dispersed into the precursor solution to obtain magnetic hydrogel inks with NP concentrations of 1.5, 2.0, and 2.5 wt%.

1.3 Two-Photon 3D Printing of Magnetically Driven Glucose-Responsive Hydrogel

To enhance adhesion between the printed microstructures and the glass substrate, 1 mL of 3-(trimethoxysilyl)propyl methacrylate (MPS) and 3 mL of acetic acid (10 v/v%, in ultrapure water) were added to 100 mL of anhydrous ethanol. O_2 Plasma-treated glass slides were immersed in the solution for 15 min, rinsed with anhydrous ethanol, and dried prior to use. The prepared hydrogel ink was drop-cast onto the silanized glass substrate and placed into a commercial two-photon 3D printer (DLW-RD, Magic NanoTech Co., Ltd., China). A 100× oil immersion objective lens (NA = 1.4, Olympus Corporation, Japan) and a femtosecond laser (780 nm) were used for voxel-by-voxel fabrication.

3D models were designed using Fusion 360 (Autodesk, Inc., USA) and sliced in Blender with a layer height and line width of 100 nm, point-to-point distance of 100 nm, and a scan speed of 4 mm/s. Laser power was adjusted within the range of 12–40 mW. To determine the minimum printable linewidth, linear patterns were fabricated at the hydrogel–substrate interface using the hydrogel ink with varying compositions. The laser power was adjusted between 40 to 16 mW. During the printing, external magnets were placed on both sides of the sample to align the Fe_3O_4 NPs. Post-printing, the samples were sequentially immersed in anhydrous ethanol, isopropanol, and n-hexane to remove unpolymerized hydrogel components.

1.4 Characterization and Performance Evaluation

1.4.1 Glucose Responsiveness Evaluation

To evaluate the glucose-responsive hydrogel, frustum-shaped microstructures (Fig. S1 a, diameter: 20 μm, height: 5 μm) supported by a cylindrical post (diameter: 8 μm, height: 5 μm), were printed and imaged using an inverted fluorescence microscope (DMI 3000, Leica Microsystems, Germany). The printed samples were

immersed in PBS and glucose solutions (varying concentrations) until fully swollen. ImageJ 2 software was used to analyze the area swelling ratio or linear expansion ratio in different solutions as a measure of glucose responsiveness. The evaluation of glucose responsiveness for K-scaffolds adopted the same procedure as described above.

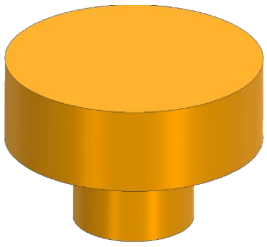

Figure S1. Three-dimensional model of the frustum-shaped microstructure.

1.4.2 Characterization

The surface morphology of the printed structures was characterized using a field-emission scanning electron microscope (FE-SEM, S-4800, Hitachi, Japan). Elemental composition and distribution were analyzed using an energy-dispersive X-ray spectroscopy (EDS) system integrated with the SEM. The magnetic properties of the printed hydrogels were measured using a vibrating sample magnetometer (VSM, 7404-S, Lake Shore Cryotronics, USA). The hydrodynamic diameter and zeta potential of the Fe_3O_4 NPs were characterized using a dynamic light scattering (DLS) instrument (NanoBrook 90Plus Zeta, Brookhaven Instruments Corporation, USA). A rotational rheometer (MCR 302, Anton Paar, Austria) was used to assess the viscosity of magnetic hydrogel inks containing various concentrations of PVP. The Young's modulus of the K-scaffolds (printed at 16, 20, 24, 28, and 32 mW) in PBS was measured using atomic force microscopy (AFM, FastScan, Bruker Corporation, Billerica, MA, USA). For each group, four parallel samples were tested (n=4). On each individual sample, force curves were acquired at five distinct locations using point-wise indentation. The data were analyzed using NanoScope Analysis software (Bruker Corporation, Billerica, MA, USA) to calculate the Young's modulus.

1.5 Magnetically Driven Motion and Embolization

At first, a multi-branch microchannel was printed by the DLW-RD printer (Magic Nano Technology Co., Ltd.) using commercial photoresist ATE-Dip 1.52 (Magic Nano Technology Co., Ltd.). Then, fetal bovine serum was added in the multi-branch microchannel, and the K-scaffold MR was positioned in the main branch of the microchannel using a micromanipulation system. Afterward, a bar permanent magnet was used to drive the K-scaffold MRs, and guide it to reach the desired embolization location. Once the MR reach this site, a 400 mM glucose solution was introduced into the medium to induce rapid expansion of the MR, thereby and occluding the targeted branch. The entire process is observed and recorded under a microscope (DMI 3000, Leica Microsystems, Germany). ImageJ 2 software was used to track the motion trajectories of the MRs.

1.6 MR-Induced Embolization in an In Vitro Vascular Model

MR were delivered into the In Vitro Vascular Model (diameter: ~65 μm) using a micromanipulation system (Leica Microsystems, Germany). Subsequently, a microsyringe pump (LSP02-1B, Longer Precision Pump Co., Ltd.) was employed to inject fresh porcine plasma (Zhengzhou Pingrui Biotechnology Co., Ltd.) containing 400 mM glucose and polystyrene (PS) microspheres (2 μm; Suzhou Nanomicro Technology Co., Ltd.) into the Vascular Model at a constant flow rate of 5 μL/min. Fresh porcine plasma was used to mimic the vascular environment, while the polystyrene microspheres served as both flow tracers and surrogate circulating cells. The entire embolization process was monitored and recorded using an optical microscope (DMI 3000, Leica Microsystems, Germany). To evaluate the embolization efficacy, the motion velocity of polystyrene (PS) microspheres before and after embolization was quantified using ImageJ 2 software, and the effectiveness was assessed by calculating the reduction rate in velocity.

1.7 Stability of Structure in porcine plasma

The MRs samples were immersed in fresh porcine plasma and incubated at 37 °C in a cell culture incubator (Midi 40, Thermo Fisher Scientific Inc.). The porcine plasma was replaced every 12 hours to maintain a physiologically relevant environment. At predetermined time points (0, 1, 2, 6, 12, 24, 48, 72, 96, and 120

hours), the structural morphology of the MRs was observed and recorded using an optical microscope (DMI 3000, Leica Microsystems, Germany). The morphological evolution and structural integrity of the MRs were analyzed over time to assess their stability under blood-mimicking conditions.

2. Formulation Optimization of Magnetic Hydrogel Inks

2.1 Determination of Monomer and Crosslinker Ratios

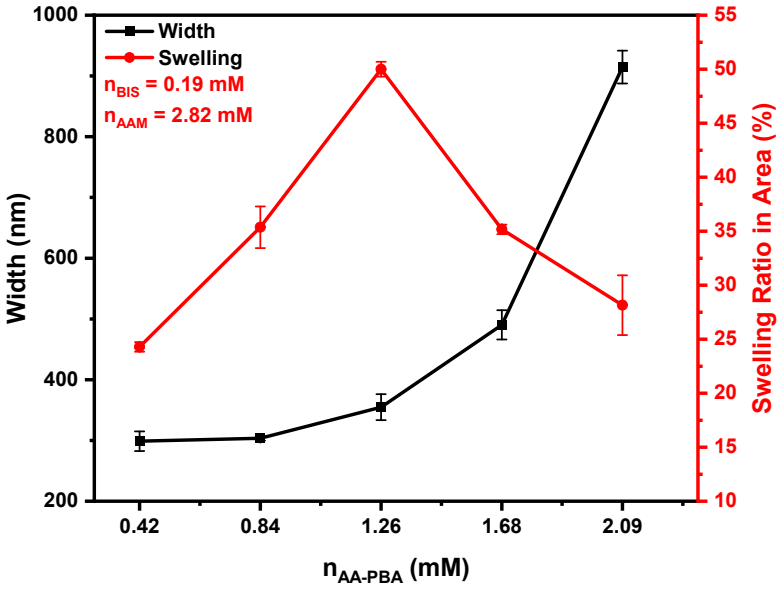

Figure S2. Effect of the glucose-responsive monomer AA-PBA concentration on the minimum printable linewidth and glucose-triggered swelling ratio of the hydrogel (n= 3).

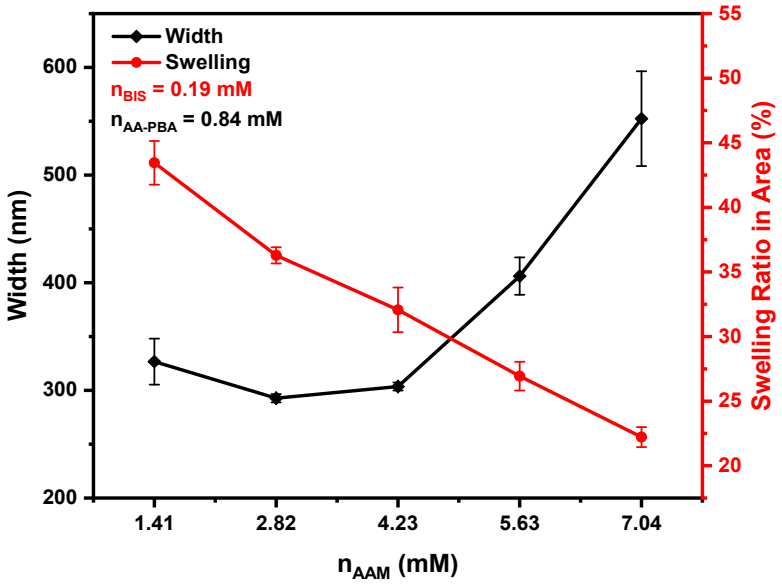

Figure S3. Effect of the hydrophilic monomer AAM concentration on the minimum printable linewidth and glucose-triggered swelling ratio of the hydrogel (n= 3).

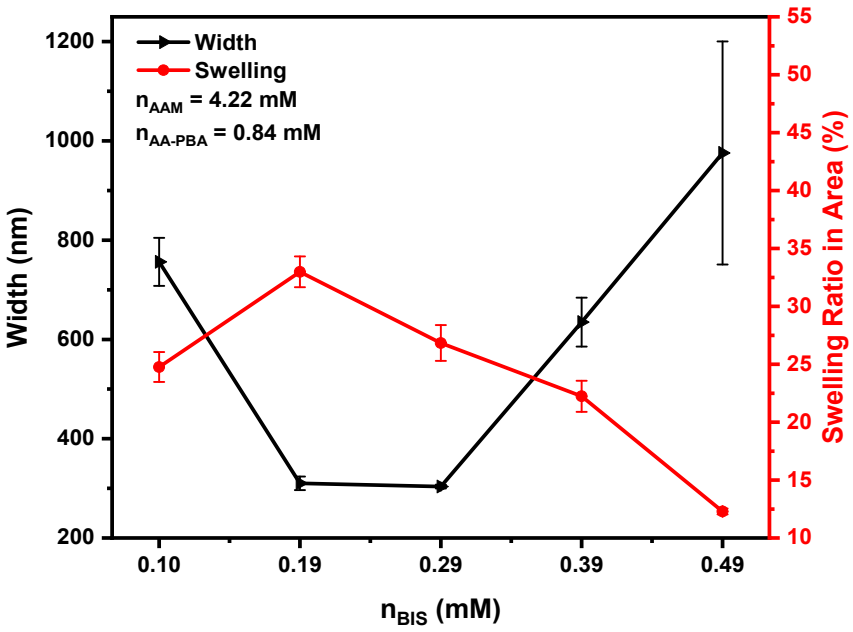

Figure S4. Effect of the crosslinker BIS concentration on the minimum printable linewidth and glucose-triggered swelling ratio of the hydrogel (n= 3).

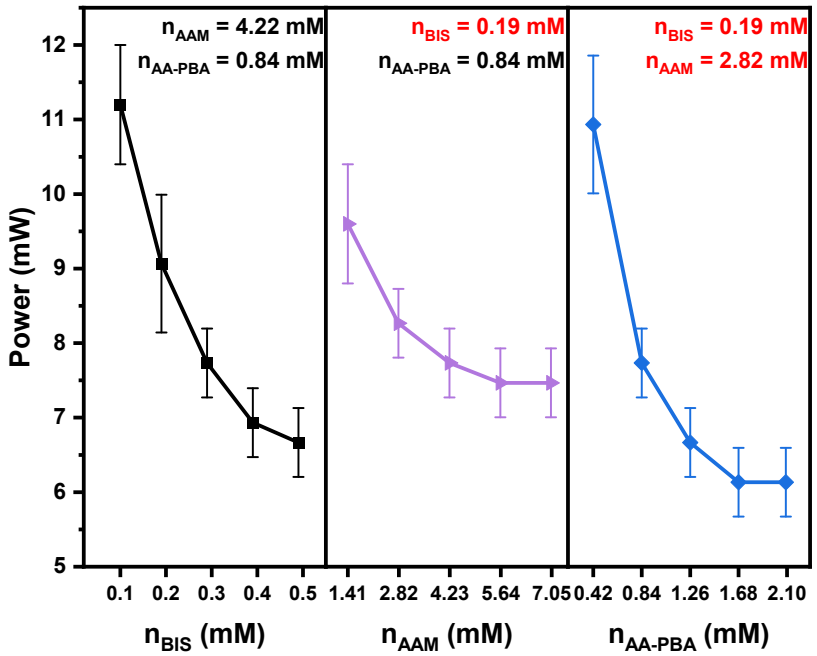

Figure S5. Influence of the concentrations of crosslinker BIS, hydrophilic monomer AAM, and glucose-responsive monomer AA-PBA on the minimum printable laser power threshold (n= 3).

2.2 Incorporation of Magnetic Fe_3O_4 Nanoparticles

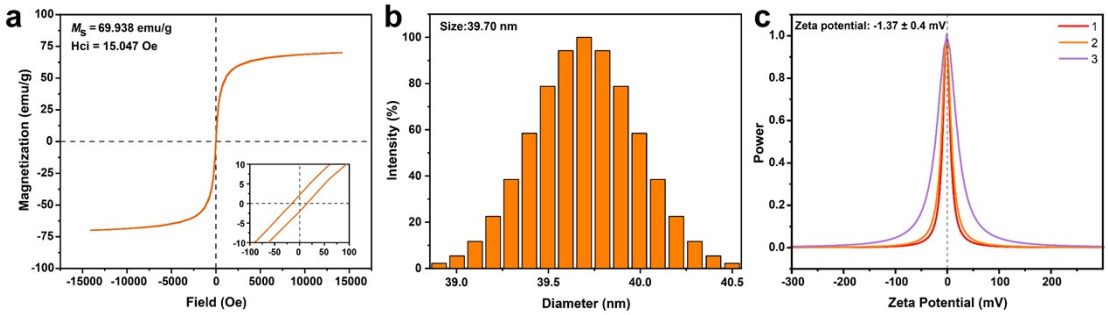

Figure S6. (a) Magnetic hysteresis loops, (b) hydrodynamic size distribution, and (c) zeta potential of the Fe_3O_4 NPs.

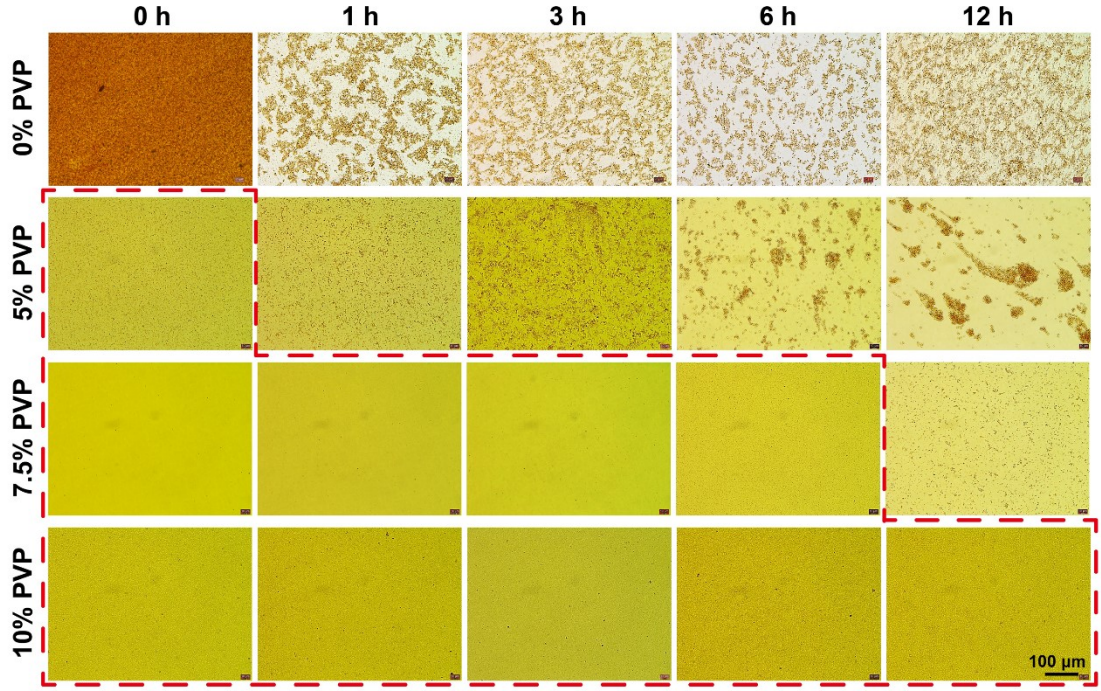

Figure S7. Optical microscopic images of the magnetic hydrogel inks containing 0%, 5%, 7.5%, and 10% PVP after resting for different durations. The section within the red dashed box indicates the inks with good dispersibility.

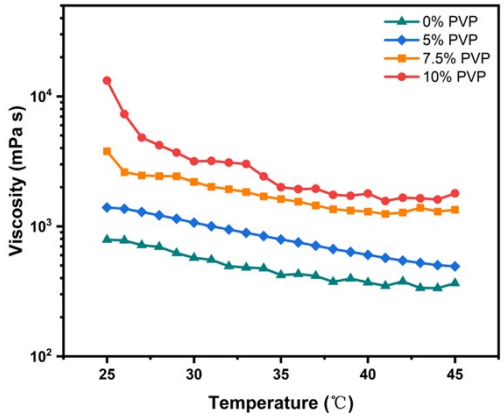

Figure S8. Temperature-dependent viscosity curves of the magnetic hydrogel inks containing 0%, 5%, 7.5%, and 10% PVP.

2.3 Design and Functional Assessment of MRs

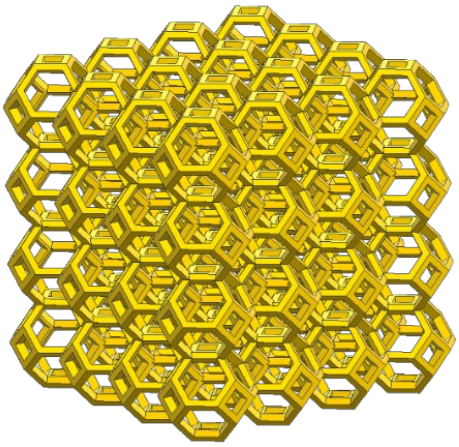

Figure S9. Three-dimensional model of magnetic glucose-responsive hydrogel K-scaffold. The K-scaffold are formed by an array of Kelvin structure elementary cells, with each cell having an approximate edge length of 5 µm. The dimensions of the K-scaffold are approximately 50 µm in length, width, and height.

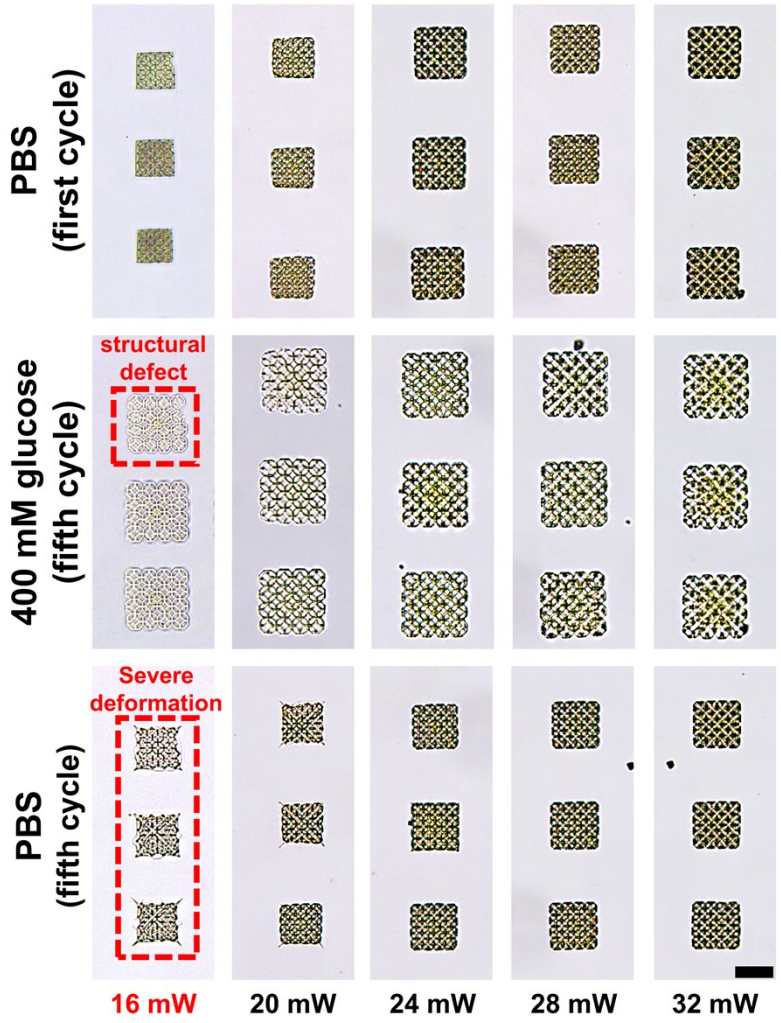

Figure S10. Optical microscopic images depicting the glucose-responsive swelling and structural stability of K-scaffolds printed under different laser powers in PBS and 400 mM glucose solution (in PBS) after fifth cycles. Scale bar: 50 µm.

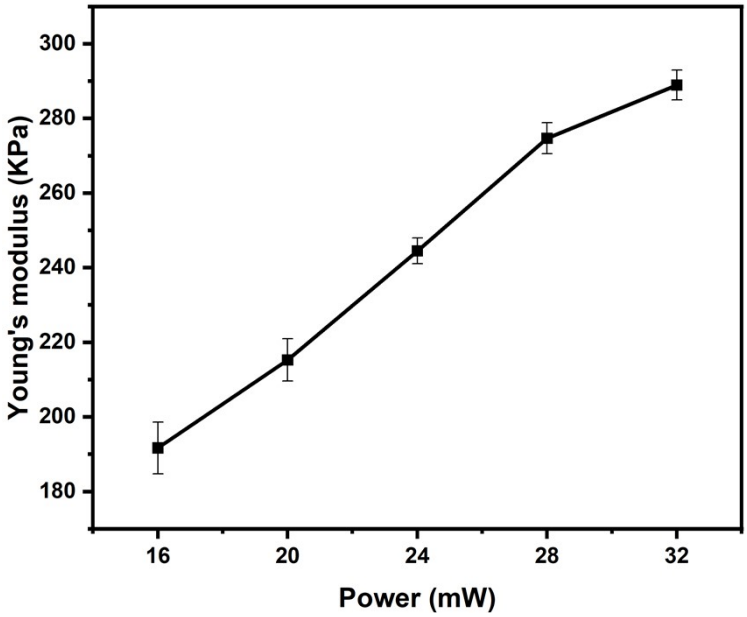

Figure S11. Young's modulus of K-scaffolds printed under different laser powers in PBS (n≥3).

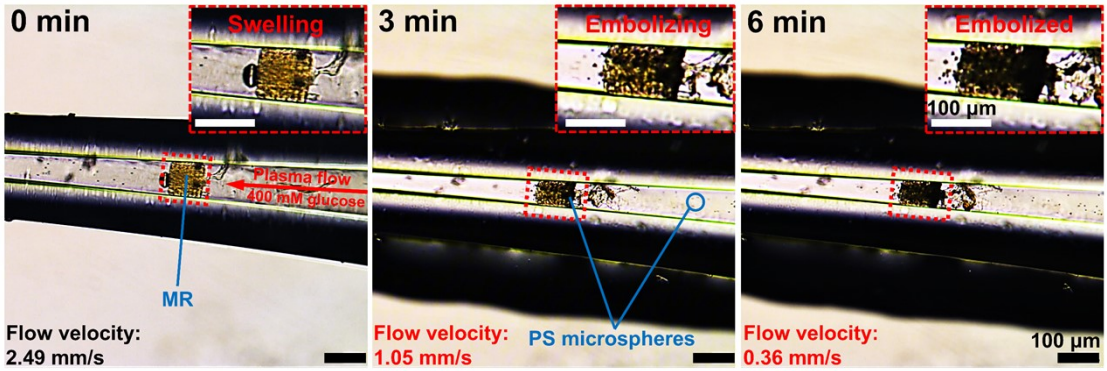

Figure S12. Time-lapse microscopic images of depicting the MR-induced embolization process in an in vitro vascular model.

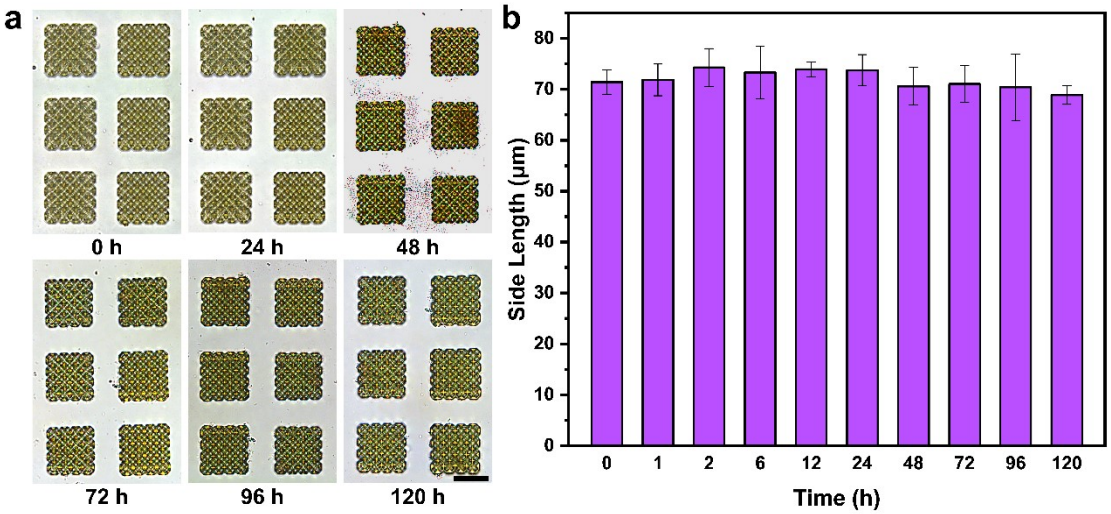

Figure S13. (a) Optical microscopyic images and (b) side lengths of MRs (printed at 20 mW) at different time points in a porcine plasma environment (n≥3.). Scale bar: 50 μm.

3. Supplementary Videos

Video S1. Swelling behavior of the K-scaffold (20 mW) upon transition from PBS to 400 mM glucose solution.

Video S2. Magnetically-guided motions of a K-scaffold MR following predefined paths, precisely delineating “W”, “U” and “T” trajectories.

Video S3. Magnetically-guided targeted motions of the K-scaffold MR in a branched microchannel filled with fetal bovine serum.

Video S4. Glucose-triggered embolization of the K-scaffold MR at the target site.

Video S5. MR-induced embolization in an in vitro vascular model.